Thermodynamic modeling of Al–Ce–Mg phase equilibria coupled with key experiments

J. Gröbner, D. Kevorkov, R. Schmid-Fetzer*

Technical University of Clausthal, Institute of Metallurgy, Robert-Koch-Str. 42 D-38678 Clausthal-Zellerfeld, Germany

Abstract

The ternary Al–Ce–Mg phase diagram was calculated using the Calphad method and investigated with selected key experiments. Arc melted alloys were annealed at 400 °C for 500 h and the phases were analyzed using quantitative X-ray powder diffraction (XRD). Differential thermal analysis (DTA) was also performed on an alloy with a composition near the ternary phase $Al_{13}CeMg_6$ (τ). Temperatures above 1000 °C could be attained due to a special sealing of the sample under argon by welding in a tantalum crucible to avoid evaporation and oxidation. Only with this procedure could reproducible and reliable DTA signals be obtained. The present experimental investigation and the consistent thermodynamic calculation show that the "ternary phase" $Ce(Mg,Al)_2$, seemingly isolated in the ternary at 400 °C, can be rationalized as a single solid solution phase between the binary end members if a larger temperature range and a solid state miscibility gap is considered. It is demonstrated that previously reported low values of ternary liquidus temperatures must be related to other phase equilibria. The actually found ternary liquidus temperatures are much higher and widely governed by the high melting compound $Ce(Al,Mg)_2$ and also by $Al_{11}Ce_3$ with primary solidification fields stretching far into the ternary system. © 2002 Elsevier Science Ltd. All rights reserved.

Keywords: A: Aluminides miscellaneous; B: Phase diagram; B: Thermodynamic and thermochemical properties; E: Phase diagram prediction (including CALPHAD)

1. Introduction

Cerium is the dominating constituent of the so called "mischmetal", an industrially used natural mixture of rare earth metals. Mischmetal is an important alloying additive for magnesium alloys. The precipitations formed as intermetallic phases with Ce in these alloys may improve the creep resistance [1] and strength at elevated temperatures. For a better understanding of the precipitating phases, the phase diagram and thermodynamics of the ternary Al–Mg–RE systems are indispensable. The related Al–Mg–Sc [2] and Al–Gd–Mg [3] systems were recently investigated in our group in an ongoing effort to generate a multicomponent thermodynamic database of magnesium alloys. The published experimental work for the Al–Ce–Mg system [4–6] gives only vertical phase diagram sections in the Al-rich corner and an isothermal section at 400 °C. Based on the experience that was made during thermodynamic calcu-

lation of the Al–Mg–Sc and Al–Gd–Mg systems, these experimental data should be carefully compared with thermodynamic data stemming from the better established binaries.

Calculation of phase equilibria and a consistency check of ternary phase analysis data with thermodynamic data of the binary subsystems require a set of Gibbs energy functions valid in the ternary system which can be obtained by the Calphad method. In addition, key experiments are identified from preliminary calculations to validate the thermodynamic models and to check possible inconsistencies in published experimental data. This combined approach of thermodynamic modeling with a minimized, though focused, experimental effort brings about an internally consistent and quantitative description of the phase equilibria in the entire ternary system, and this is the purpose of the present study.

2. Experimental information in the literature

The first partial phase diagram of the Al–Ce–Mg system was published by [4]. They prepared 16 binary and

* Corresponding author. Tel.: +49-5323-72-2150; fax: +49-5323-72-3120.

E-mail address: schmid-fetzer@tu-clausthal.de (R. Schmid-Fetzer).

57 ternary alloys in the Ce-poor region between 0 and 33.3 at.% Ce. The metals were melted in alumina crucibles in an electrical resitance furnace under a eutectic mixture of KCl and LiCl. The alloys were annealed in evacuated glass ampoules at 400 °C for 350 h, quenched in cold toluene and analysed by X-ray diffraction. Only a partial isothermal section at 400 °C was given by [4]. A solubility of Al in $CeMg_{12}$ at about 5 at.% Al and a ternary Laves-phase crystallising in the hexagonal $MgZn_2$-structure with $a = 0.552$ pm and $c = 0.889$ pm was found [4]. Cui et al. [7] reported additionally two new ternary phases with peculiar compositions, Al_4CeMg_4 and $Al_{21}CeMg_8$. [8] gives a small part of the Al-rich liquidus surface and one ternary reaction $L = (Al) + Al_{11}Ce_3 + \beta$ at 446 °C.

A complete isothermal section at 400 °C of the system Al–Ce–Mg was given by [5]. They prepared the alloys in the same way as [4] and annealed them in evacuated silica tubes for 480 h at 400 °C. They found a large solubility of Al in the phases $CeMg_2$ (ap. 46 at.%), CeMg (approx. 30 at.%) and confirmed the Al-solution in the $CeMg_{12}$ phase. Al_2Ce dissolved about 5 at.% Mg. Most of the tie lines are connected with this stable phase [5]. There is a contradiction with the binary phase diagram Ce–Mg [9] in which the phase $CeMg_2$ is not stable at 400 °C. According to their experimental results this phase decomposes at 615 °C and is stable only at higher temperatures.

The same experimental results of [5] combined with thermoanalytical measurements were used to derive four pseudobinary sections, a partial liquidus surface and seven ternary invariant reactions [6]. They confirmed the existence and the crystal structure of the ternary phase reported by [4] with slightly different lattice parameters ($a = 0.531$ pm and $c = 0.894$ pm). The composition of this phase is given as $Al_2Ce_{0.15}Mg_{0.85}$ and a congruent melting temperature for this phase is claimed at 635 °C. The temperatures and compositions of invariant reactions given by [6] will be detailed later.

3. Present experimental investigation

3.1. Methods

Four alloys were prepared as key experiments to check the calculated phase equilibria and to provide the missing high temperature data indicated by the new interpretation of the liquidus temperatures based on the thermodynamic calculation. The alloys were carefully arc melted under purified argon to avoid extensive evaporation of Mg and Al. Starting materials were Ce bulk (99.9 wt.% Auer-Remy, Hamburg), Al powder (99.8 wt.% Alfa, Karlsruhe) and Mg pieces (99.98 wt.% Alfa, Karlsruhe). The loss in total mass was below 3% for all samples that went to further analysis. The melted samples were sealed in silica tubes and annealed at 400 °C for three weeks (500 h). After rapid cooling in water the alloys were powdered in a steel ball mill for investigation by X-ray powder diffraction analysis (XRD) to determine the phases present. The measurements were performed using a Siemens D5000 diffractometer with a step 0.02° of 2Θ and 3 s exposition time in the point. The obtained diffraction patterns were analyzed quantitatively using the program PowderCell 2.1 [10].

Thermal analysis was performed on one alloy (Al65–Ce5–Mg30, at.%) with a composition near the ternary phase using a Netzsch DTA 404 apparatus. The premolten sample was sealed under argon by welding in a thin-walled tantalum crucible to avoid evaporation and oxidation. The DTA measurements were carried out with heating/cooling rate of 5 K/min and under vacuum to protect the Ta-crucible. The sample was heated and cooled 2 times for the precise determination of peak positions. The estimated error of measurements is ±5 K. Difference between heating and cooling peaks was lower than 4 K. After the DTA measurements the sample was investigated again by XRD.

3.2. Experimental results

Results of the XRD phase analysis are presented in Table 1. The phase contents of all samples show good agreement with the expected ones from the thermodynamic calculation, as given in Fig. 1, and confirm the triangulation and ternary solubilities of [4,5].

The "ternary phase" $Ce(Mg,Al)_2$, seemingly isolated in the ternary at 400 °C, can be rationalized as a single solid solution phase between the binary end members if a larger temperature range is considered. The binary $CeMg_2$ is stable from 615 to 747 °C [9], and the binary $CeAl_2$ from room temperature to 1480 °C [11] and they all have the same crystal structure as the $Ce(Mg,Al)_2$,

Table 1
Alloys annealed at 400 °C for 3 weeks and phases observed by XRD. Solubilities calculated using Vegard's law and the data of [5]

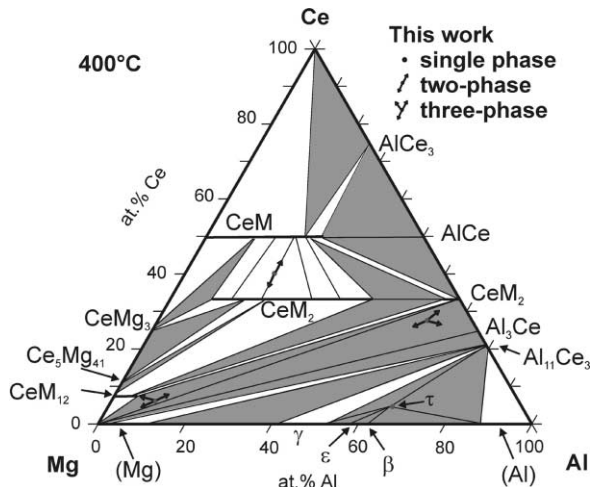| Alloy composition (at.%)	Phases	Lattice constant (nm)	Phase composition (at.%)
Al20Ce40Mg40	Ce(Mg,Al)	$a = 0.385$	Al15Ce50Mg35
	$Ce(Mg,Al)_2$	$a = 0.850$	Al15Ce33Mg52
Al62Ce28Mg10	$Ce(Mg,Al)_2$	$a = 0.808$	Al62Ce33Mg5
	Al_3Ce		
	(Mg)		
Al10Ce5Mg85	$Ce(Mg,Al)_2$	$a = 0.808$	Al62Ce33Mg5
	$Ce(Mg,Al)_{12}$	$a = 1.043$	Al5Ce8Mg87
		$c = 0.596$	
	(Mg)		
Al65Ce5Mg30	τ ($Al_{13}CeMg_6$)		
	$Al_{11}Ce_3$		
	(Al) ?		

Fig. 1. Calculated isothermal section at 400 °C including compositions of own samples. $CeM_x = Ce(Mg,Al)_x$. Dots represent the investigated sample compositions, arrows point towards the identified phases. Three-phase triangles are shaded. The calculation is also supported by the experimental data of [4,5].

observed in the ternary at 400 °C. This phase is therefore designated with the unique symbol CeM_2 in Table 2 and Fig. 1, where it exists inside the ternary as well as extending from the binary $CeAl_2$ with a miscibility gap in between. In Table 2 all solid phases existing with a ternary composition are compiled and the other two solution phases originating from CeMg and $CeMg_{12}$ are designated analogously as CeM and CeM_{12}. Both these solutions, however, do not have a stable end member at the Ce–Al side at any temperature.

For the phases CeM, CeM_2 and CeM_{12} large variations of the measured d-values were observed. The corresponding compositions given in Table 1 were calculated using the linear d-value/composition relation reported by [5]. The ternary phase $Al_{13}CeMg_6$ (τ) and the binary phases Al_3Ce and $Al_{11}Ce_3$ show no differences to the d-values calculated from their given crystal structure. Therefore no solubility was assumed for these phases.

Three thermal signals were observed during the DTA heating runs of the alloy with a composition near the ternary phase: at 455, 509 and 926 °C. For the first signal the onset was taken since it is related to a non-variant reaction, whereas the peak maximum was taken for the liquidus point at 926 °C. On cooling the signal for the liquidus was too small for extracting, the other reactions showed an undercooling of 3 °C. Only the heating signals were considered as close to equilibrium and used for a comparison. Table 3 compares the experimentally observed invariant equilibria of the ternary Al–Ce–Mg system with the calculated ones and the reported reactions of [6]. It also shows the type of reactions observed at 453 °C.

4. Thermodynamic modeling

The present modeling of the ternary phase equilibria is based on the binary thermodynamic datasets of the subsystems Ce–Mg [9], Al–Mg [13] and an update [11] of the Al–Ce system [12]. It is noted that this data set for Al–Ce shows an inverted miscibility gap in the liquid phase above 2500 °C, which is considered to be artificial.

The Gibbs energy function $G_i^{0,\phi}(T) = G_i^\phi(T) - H_i^{SER}$ for the element i ($i = $ Al, Ce, Mg) in the ϕ phase ($\phi = $ fcc (Al, γCe), bcc (δCe) and hcp (Mg), or liquid) is described by the equation:

$$
\begin{aligned}
G_i^{0,\phi}(T) = {} & a + b \cdot T + c \cdot T \cdot \ln T + d \cdot T^2 + e \cdot T^3 \\
& + f \cdot T^{-1} + g \cdot T^7 + h \cdot T^{-9}
\end{aligned} \tag{1}
$$

where H_i^{SER} is the molar enthalpy of the stable element reference (SER) at 298.15 K and 1 bar, and T is the absolute temperature. The Gibbs energy functions for Al, Ce and Mg are taken from the SGTE compilation by Dinsdale [14].

The liquid, fcc (Al, γCe), bcc (δCe) and hcp (Mg) solution phases are described by the substitutional

Table 2
The solid phases existing inside the ternary system

Phase symbol	Phase description	Composition range at 400 °C (at.% Al)	Structure type	Pearson symbol / space group	Lattice parameter (nm)	Reference
CeM	$Ce(Mg,Al)_1$	0–30	CsCl	cP2 $Pm\bar{3}m$	$a = 0.3882$–0.383	[5]
CeM_2	$Ce(Mg,Al)_2$	10–46 and 61–66.7 (0–66.7)[a]	$MgCu_2$	cF24 $Fd\bar{3}m$	$a = 0.870$–0.815 and $a = 0.808$–0.770	[5], this work
CeM_{12}	$Ce(Mg,Al)_{12}$	0–5	$ThMn_{12}$	tI26 $I4/m$	$a = 1.033$ $c = 0.596$	[4]
τ	$Al_{13}CeMg_6$	Stoichiometric	$MgZn_2$	hP12 $P6_3/mmc$	$a = 0.533$ $c = 0.8940$	[5]

[a] At 740 °C, this work.

Table 3
Calculated and measured temperatures and liquid compositions of invariant reactions

Reaction	Type	Calculated (this work)			Measured (this work)	Measured [6]		
		T in °C	at.% Al	at.% Ce	T in °C	T in °C	at.% Al	at.% Ce
$L + CeM_2 + \beta Al_{11}Ce_3 + \alpha Al_{11}Ce_3$	D_1	1020	55.7	7.6				
$L = CeM + CeM_2$	max	906	18.7	68.9				
$L + CeM_2 = CeM + AlCe$	U_1	817	34.3	64.2				
$L = CeM + AlCe_3$	max	676	24.9	74.3				
$L = CeM + AlCe + AlCe_3$	E_1	664	28.7	70.9				
$L + \delta Ce = CeM + \gamma Ce$	U_2	620	9.6	87.3				
$L + Ce_5Mg_{41} = CeM_2 + Ce_2Mg_{17}$	U_3	614	<0.01	7.5				
$L + CeM_2 = Ce_2Mg_{17} + CeM_{12}$	U_4	613	<0.01	7.2				
$L = CeM_2 + (Mg)$	max	604	3.7	2.1		599	[a]	6.6
$L + CeM_2 = CeM_2' + (Mg)$	U_5	598	6.7	1.4				
$L + CeM_2 = (Mg) + CeM_{12}$	U_6	597	1.4	3.4				
$L = CeM + \gamma Ce + AlCe_3$	E_2	577	13.8	85.1				
$L + CeM_2 = \alpha Al_{11}Ce_3 + (Mg)$	U_7	561	14.7	0.3				
$L = \gamma + \alpha Al_{11}Ce_3$	max	463	47.1	<0.01		445	46.7	2.6
$L = \tau + \alpha Al_{11}Ce_3$	max	455	62.2	<0.01		490	68.7	7.9
$L + \alpha Al_{11}Ce_3 = (Al) + \tau$	U_8	453	64.2	<0.01	455	445	82.2	4.0
$L + \alpha Al_{11}Ce_3 = \gamma + \tau$	U_9	452	56.4	<0.01		440	52.1	5.1
$L = \beta + \tau$	max	451	60.3	<0.01		444	61.6	1.6
$L = (Al) + \beta + \tau$	E_3	450	63.8	<0.01		441[b]	63.5	1.0
$L = \beta + \gamma + \tau$	E_4	449	57.6	<0.01		442	56.2	1.1
$L = \gamma + \alpha Al_{11}Ce_3 + (Mg)$	E_5	436	31.0	<0.01		436	25.0	4.0

[a] Data reported in table (22.6 at.% Al) and figure (19.0 at.% Al) are contradictory [6] and were presumably obtained from graphical extrapolation of DTA data points [6], see also Fig. 5.
[b] Previously reported as $L = (Al) + \beta + Al_{11}Ce_3$ at 446 °C [8].

solution model. For the liquid phase the molar Gibbs energy is expressed by following equation:

$$
\begin{aligned}
G^{Liq} =\ & x_{Ce}G_{Ce}^{0,Liq} + x_{Mg}G_{Mg}^{0,Liq} \\
& + RT\big(x_{Ce}\ln x_{Ce} + x_{Mg}\ln x_{Mg}\big) \\
& + x_{Ce}x_{Mg}\big(L_{Ce,Mg}^{0,Liq} \\
& + L_{Ce,Mg}^{1,Liq}(x_{Ce} - x_{Mg}) + L_{Ce,Mg}^{2,Liq}(x_{Ce} - x_{Mg})^2 + ...\big)
\end{aligned}
\tag{2}
$$

in which R is the gas constant, and x_{Ce} and x_{Mg} are the molar fraction of Ce and Mg. The interaction parameters L^0, L^1 and L^2 may be linearly temperature dependent and are taken from the optimized binary datasets. Using the Redlich-Kister type Eq. (2) also for ternary compositions without introducing ternary interaction parameters, is equivalent to in the widely used Muggianu extrapolation of the thermodynamic data.

A preliminary calculation using only this extrapolation of binary data into the ternary reproduces already the essential features of the isothermal section at 400 °C reported by [4] and [5] and confirmed by own samples. The eutectic temperature in the vertical section Al₂Ce–Mg found at 599 °C by [6] is reproduced only 5 K higher without using any ternary parameter for the liquid. Therefore no ternary interaction parameter was

used for the calculation. All calculations were done using the Pandat program [15,16].

As detailed in Section 3.2 the binary phases CeAl₂ and CeMg₂, crystallizing in the same crystal structure (Cu₂Mg), are rationalized as a continuous solid solution with a miscibility gap at lower temperature. This phase was modeled with two sublattices and a substitutional solution on the second sublattice, $Ce_1(Al,Mg)_2$, called CeM₂. Similarly, the other two ternary solutions of binary phases are modeled as $Ce_1(Al,Mg)_z$ with $z = 1$ and 12. The Gibbs energy of the phases CeM$_z$ (per mole of atoms) is expressed by

$$
\begin{aligned}
G^{\phi} =\ & y_{Al}G_{Ce:Al}^{0,\phi} + y_{Mg}G_{Ce:Mg}^{0,\phi} \\
& + \frac{vz}{1+z} \cdot R \cdot T\big(y_{Al} \cdot \ln y_{Al} + y_{Mg} \cdot \ln y_{Mg}\big) \\
& + y_{Al} \cdot y_{Mg} \cdot \big(L_{Ce:Al,Mg}^{0,\phi} + (y_{Al} - y_{Mg}) \cdot L_{Ce:Al,Mg}^{1,\phi} + ...\big)
\end{aligned}
\tag{3}
$$

in which y_{Al} and y_{Mg} are the site fractions of Al and Mg on the second sublattice. The parameters $G_{Ce:*}^{0,\phi}$ (also called compound energies) are expressed relative to the Gibbs energies of the pure elements (Ce-hcp, Al-fcc, Mg-hcp) at the same temperatures and represent, for $z = 2$, the stable binary CeMg₂ and CeAl₂ phases. The values are taken from the binary description of the

Ce–Mg [9] and Al–Ce [11] systems. The L^0 and L^1 parameters are actual ternary interaction parameters, optimized in the present study.

For the two phases CeMg (CeM) and CeMg$_{12}$ (CeM$_{12}$) with limited ternary solution ranges, the parameters $G_{Ce:Al}^{0,\phi}$ represent the metastable end members of the solid solutions in the binary Al–Ce system. They were given sufficiently large positive values in this work. Therefore, Mg becomes the main consituent on the second sublattice of these two phases. AlCe is not an end member of the solution CeM. It is modeled as a separate phase because of its different crystal structure. The parameter for the ternary phase Al$_{13}$CeMg$_6$ (τ) was determined according to the observed solid state equilibria and the nonvariant reaction $(L = \tau + (Al) + Al_{11}Ce_3)$ which was measured at 455 °C.

The calculated isothermal section of the Al–Ce–Mg system at 400 °C is given in Fig. 1. The investigated sample compositions are shown and the number of phase observed is indicated. The arrows point towards the measured phase compositions. The calculated

vertical zsection along the one-phase field CeM$_2$ is given in Fig. 2. It is almost a pseudobinary system, except for the low temperature decomposition part around CeMg$_2$. The miscibility gap on the CeAl$_2$-rich side below 733 °C compares well with the experimental data of [5]. The calculated liquidus surface is shown in Fig. 3. It is dominated by the stable phase CeM$_2$. The composition of this phase is marked by the dashed line. The
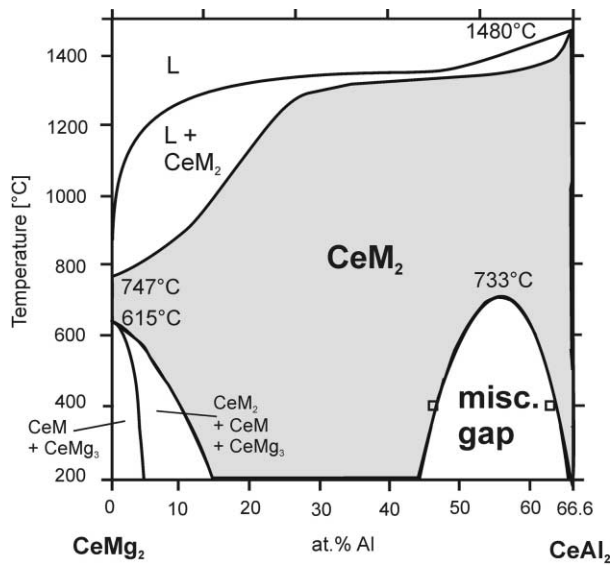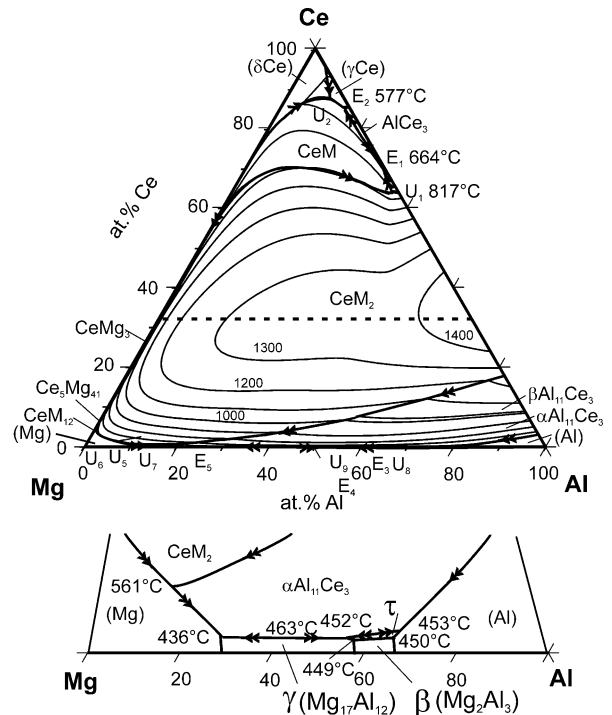

Fig. 3. Calculated liquidus surface including isotherms. The Al–Mg edge is shown in schematic enlargements.

Fig. 2. Calculated vertical section CeMg$_2$–CeAl$_2$ with experimental data [5].

Table 4
Assessed ternary parameters for the Al–Ce–Mg system in J/mol of formula unit

$G_{Ce:Al}^{CeM} = -50000 + G_{Al}^{0,fcc} + G_{Ce}^{0,fcc}$

$L_{Ce:Al,Mg}^{0,CeM} = -160000 + 100*T$

$G_{Ce:Al}^{CeM12} = -100000 + 12*G_{Al}^{0,fcc} + G_{Ce}^{0,fcc}$

$L_{Ce:Al,Mg}^{0,CeM12} = -80000$

$L_{Ce:Al,Mg}^{0,CeM2} = -22000 + 10*T$

$L_{Ce:Al,Mg}^{1,CeM2} = +16000$

$G_{Al:Ce:Mg}^{Al13CeMg6} = -214000 + 10*T + 13*G_{Al}^{0,fcc} + G_{Ce}^{0,fcc} + 6*G_{Mg}^{0,hcp}$
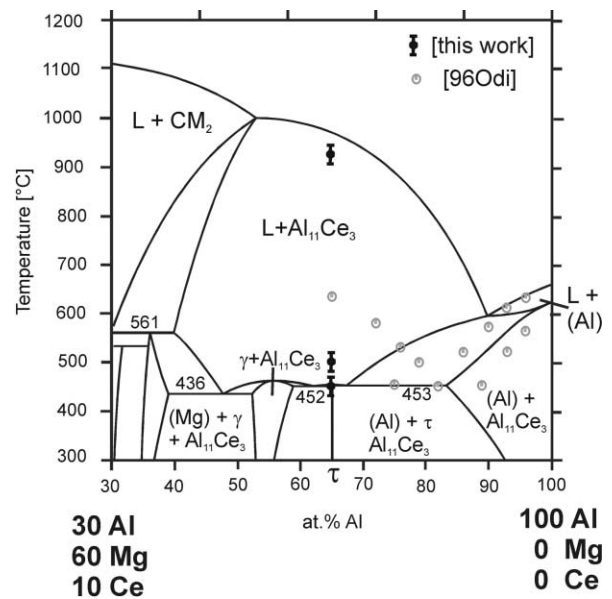

Fig. 4. Calculated vertical section including our own DTA results and those of [6].

assessed ternary thermodynamic parameters of the Al–Ce–Mg system are given in Table 4.

5. Discussion

Fig. 4 gives the calculated vertical section through the ternary system Al–Mg–Ce containing pure Al and the ternary phase τ. The present DTA results and the data of [6] are also indicated. The three thermal signals measured in this work refer to a sample composition of τ (nominal Al 65–Ce 5–Mg 30 at.%). According to our experience the observed weight loss of maximum 3% during preparation is to be assigned essentially to Mg-evaporation. The corresponding maximum composition shift is Al 67.6–Ce 5.2–Mg 27.2 at.%. This is also supported by the observation of a small amount of $Al_{11}Ce_3$ and traces of (Al) in a sample of that nominal composition, see Table 1 and compare to Fig. 1. The data in Fig. 4 should be judged keeping this sample shift towards higher Al-composition in mind.

The perfect fit of measurement and calculation at the nonvariant reaction at 455 °C is a result of the modeling of the phase τ, but most notable is the reasonable agreement at the liquidus temperature of 926 °C. The intermediate signal at 509 °C is small and cannot be accounted for. It is emphasized that the high liquidus temperature calculated at 971 °C (for the nominal composition of τ) is a result of straightforward calculation from the binary data without any ternary parameter. Since only the phases $L + Al_{11}Ce_3$ are involved, and $Al_{11}Ce_3$ is a stoichiometric binary phase, this key experiment provides a true check of the validity of the extrapolation of the binary data of the liquid phase using Eq. (2). The agreement between calculated and

measured liquidus of 926 °C is considered as reasonable and the difference of 45 K gives an idea of the accuracy of the predicted ternary liquidus temperatures in that area. The error may actually be smaller because of the sample shift towards higher Al-composition.

This fact clearly shows that the previous interpretation of the data of [6] in Fig. 4 as "liquidus temperatures", 300 K below the present measurement, cannot be accepted. They may not have measured up to such high temperatures, which is not a trivial task. In fact, our experience with this system and related Mg–Al–Gd,Sc systems shows that reliable high temperature DTA data can only be obtained using hermetically sealed inert crucibles to avoid evaporation and oxidation. We have used suitable in-house made thin-walled tantalum capsules for that purpose. Experimental details were not reported in [5,6].

In Fig. 5 the calculated vertical section $CeAl_2$–Mg is given including the data points of [6]. This section is not a pseudobinary phase diagram as assumed by [6]. Again, good agreement is observed concerning the invariant temperature (598 °C) but the temperatures interpreted as liquidus by [6] are substantially below the calculated liquidus of CeM_2. The low temperature signals around 400 °C cannot be accounted for and were also disregarded in the original interpretation [6]

It was shown above that the reported "congruent melting point at 635 °C" [6] of the ternary phase could not be confirmed by our measurements. If the thermal stability of τ was modeled such that an incongruent decomposition at 635 °C is obtained, a conflict would arise with the experimentally observed solid state equilibria at 400 °C: the higher stability of τ would produce tie lines with Al_3Ce or even CeM_2 in contrast with reality.

Also the pseudobinary character of the sections Al–τ, Al_2Ce–Mg, τ–β and τ–γ reported by [6] on the base of their DTA analysis is in contradiction to the thermodynamic calculations. The invariant reaction equations and temperatures of [6], however, agree reasonably with the calculated multi-phase equilibria given in Table 3. The large Ce-contents of 1–7.9 at.% Ce, however, concluded from the graphical interpretation of the DTA data of [6], cannot be accepted. Addition of trace amounts of cerium (calculated > 0.01 at.% Ce) to Mg–Al alloys with 30–70 at.% Al results in primary precipitation of $Al_{11}Ce_3$ and the entire collection of invariant reactions in that range is almost degenerate to the binary Mg–Al system as also seen from the liquidus surface in Fig. 3.

The high liquidus temperatures are a consequence of the large thermodynamic stability of the solid Al–Ce phases $Al_{11}Ce_3$ and $AlCe_2$ (CeM_2) that produce dominating fields of primary crystallization of these phases. The corresponding liquidus surface in Fig. 3 is steeply rising from the binary Mg–Al edge upon addition of
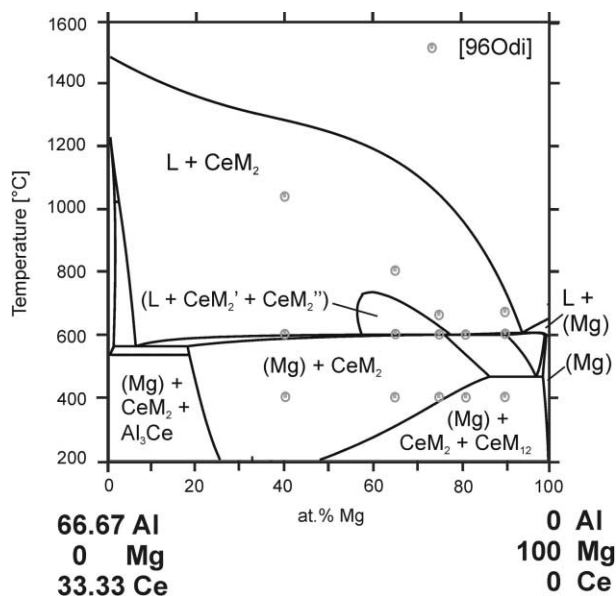

Fig. 5. Calculated vertical section $CeAl_2$–Mg including the data of [6].

cerium. It is emphasized again that this is a direct consequence of the thermodynamic data of the binary phases and not influenced by ternary modeling. In the schematically enlarged Mg–Al edge in Fig. 3 the very narrow field of primary crystallization of the ternary phase τ is given, which is cut off at higher Ce-content by that of the $Al_{11}Ce_3$ phase, thus rendering the ternary phase τ as incongruent melting.

The isothermal section at 400 °C given in Fig. 1 fits excellently to that reported by [5]. The $CeMg_2$ phase is not stable in the binary subsystem Ce–Mg at this temperature but it is stabilized by Al in the ternary system. The solid solution between $CeMg_2$ and Al_2Ce, named CeM_2 in this work, is calculated to be complete above the critical temperature of the miscibility gap at about 733 °C and below the binary peritectic decomposition of $CeMg_2$ at 747 °C (Fig. 2).

6. Conclusions

The ternary phase diagram Al–Ce–Mg was calculated using no other ternary parameter than that for the Gibbs energy of the ternary phase $Al_{13}CeMg_6$ (τ) and for the ternary solubilities of the binary phases. The present experimental investigation and the consistent thermodynamic calculation show that the "ternary phase" $Ce(Mg,Al)_2$, seemingly isolated in the ternary at 400 °C, can be rationalized as a single solid solution phase between the binary end members if a larger temperature range is considered. The extrapolation of the binary data sets produce a satisfying agreement with experimental data, indicating well defined Gibbs energy data sets of the binary phases.

Previous thermal analysis data interpreted as very low liquidus temperatures [6] are shown to contradict other experimental results and the thermodynamic data. Because of the high enthalpies of formation and quite normal entropies of the binary Al–Ce phases $Al_{11}Ce_3$ and Al_2Ce the liquidus should be much higher than assumed by [6]. One of the present key experiments defined from that thermodynamic result was to perform the DTA measurement up to much higher temperatures. This was realized by a special encapsulation technique of the sample. In fact, a liquidus point at ~926 °C was detected, much higher than the measurement range of [6]. The lower invariant reaction temperatures of [6], as well as the isothermal triangulation of [5] and [4] agree well with the calculated phase diagram. The invariant reactions of the Ce-poor part of the liquidus surface of [6] and the ternary reaction of [8] also agree with the calculation. These reactions, however, are virtually degenerate to the binary Al–Mg system as detailed in Table 3. Other ternary phases reported by [7] were not confirmed.

It is remarkable that similar contradictions were also found in other related systems. In recently published investigations in the Al–Mg–Sc [2] and in the Al–Gd–Mg system [3] liquidus temperatures were found substantially higher than reported in the related literature. A similar trend is supposed in ternary Al–Mg systems with RE or Y. Here the DTA results interpreted as liquidus temperatures are also not in agreement with the known large enthalpies of formation of Al_2RE phases. It becomes apparent that in such complex systems it is essential to support the interpretation of thermoanalytical measurements by thermodynamic calculations. Further work in some of those systems is currently in progress.

References

[1] Pettersen G, Westengen H, Høier R, Lohne O. Microstructure of a pressure die cast magnesium-4 wt.% aluminium alloy modified with rare earth additions. Mater Science Eng 1996;A207: 115–20.

[2] Gröbner J, Schmid-Fetzer R, Pisch A, Cacciamani G, Riani P, Ferro R. Experimental investigations and thermodynamic calculation in the Al–Mg–Sc system. Z Metallkd 1999;90:872–80.

[3] Gröbner J, Kevorkov D, Schmid-Fetzer R. Thermodynamic calculation of Al–Gd and Al–Gd–Mg phase equilibria checked by key experiments. Z Metallkd 2001;92:22–7.

[4] Zarechnyuk OS, Kripyakevich PI. X-Ray structural investigation of the Ce–Mg–Al system in the range 0–33.3 at.% Ce. Russ Metall 1967;4:101–3.

[5] Odinaev KO, Ganiev IN, Kinzybalo VV, Kurbanov HR. Phase equilibria in the Al–Mg–Y and Al–Mg–Ce systems at 673 K. Izv vyssich ucebnych zavedenij, Cvetnaja metallurgija 1989;2:75–7.

[6] Odinaev KO, Ganiev IN, Ikromov AZ. Pseudobinary sections and liquidus surface of the Al–Mg–CeAl₂ system. Russ Metall 1996;3:122–5.

[7] Cui Z, Wu R. Phase diagram and properties of ternary Al–Mg–Ce alloys. Acta Metallurgica Sinica 1984;20(6):B323–31.

[8] Zheng C, Wu Y, Qian J, Ye Y. Liquidus and intermetallic compound in Al-rich region of Al–Mg–Ce system. Acta Metallurgica Sinica 1986;22(2):B63–7

[9] Cacciamani, G., Borzone, G., Ferro, R.. System Ce–Mg. In Ansara I, Dinsdale AT, Rand MH, editors. COST507—thermochemical database for light metal alloys, July 1998. European Commission EUR 18499 EN, p. 137–40.

[10] Kraus W, Nolze G. Powder Cell for Windows, Version 2.1, 15.02.1999. Federal Institute for Materials Research and Testing, BAM, Germany; 1999.

[11] Cacciamani G. Modified data set of Al–Ce, priv. communication, 1999.

[12] Cacciamani G, Borzone G, Ferro R. System Al–Ce. In: Ansara I, Dinsdale AT, Rand MH, editors. COST507—thermochemical database for light metal alloys, July 1998. European Commission EUR 18499 EN, p. 20–2.

[13] Liang P, Su H-L, Donnadieu P, Harmelin MG, Quivy A, Ochin P, et al. Experimental investigation and thermodynamic calculation of the central part of the Mg–Al phase diagram. Z Metallkd 1998;89(8):536–40.

[14] Dinsdale AT. Thermochemical data of the elements. CALPHAD 1991;15:317–425.

[15] Pandat—phase diagram calculation engine for multicomponent systems. CompuTherm LLC, 437 S. Yellowstone Dr., Suite 217, Madison, Wisconsin, USA (2000).

[16] Chen S-L, Daniels S, Zang F, Chang YA, Oates WA, Schmid-Fetzer R. On the calculation of multicomponent stable phase diagrams. J Phase Equilibria 2001;22:373–8.